DINAME 2023 - Proceedings of the XIX International Symposium on Dynamic Problems of Mechanics,
A.S. De Paula, A.T. Fabro and M.R. Machado (Editors), ABCM.
Pirenópolis, Go, Brazil, February 26th to March 3rd, 2023

Design of a Flexible Monopile Foundation for the Offshore Wind Turbine Vibration Control by Pendulum Tuned Mass Dampers

Gino Bertollucci Colherinhas[1], Marlipe Garcia Fagundes Neto[1], Sigeo Kitatani Júnior[1], and Marcus Vinicius Girão de Morais[2]

[1] Universidade Federal de Goiás, Campus Samambaia, Escola de Engenharia Mecânica (EMC), Av. Ingá, Prédio B5, 70910900 - Goiânia/GO, Brasil. {gino;marlipe;sigeojr}@ufg.br

[2] Universidade de Brasília, Campus Darcy Ribeiro, Faculdade de Tecnologia, Bloco G, Asa Norte, 70910-900 - Brasília/DF, Brasil. mvmorais@unb.br

Abstract: In this study, a flexible monopile foundation is modeled considering the Pile-Soil Interaction (PSI) enhancing a previously designed Offshore Wind Turbine (OWT) model controlled by an optimal passive-adaptive Pendulum-Tuned Mass Damper (PTMD). The PSI is designed by a pile modeled as beam-column elements supported by nonlinear springs for lateral loads (p-y curves) and axial loads (t-z and Q-z curves), applied at the nodal points between the elements. The estimation of wind and wave spectra, as well as the hydrodynamic and aerodynamic loads, are conducted by using an in-house built MATLAB® routine working together with an ANSYS® 3-D finite element (FE) global model for evaluating the resultant peak displacement response at the OWT hub by a power spectral density (PSD) analysis. This procedure basis on the 5-MW baseline OWT proposed by the National Renewable Energy Lab (NREL). A selected design case of PTMD parameters compares the PSD response with and without soil interaction and an static analysis procedure evaluates the monopile displacements and stresses along the pile.

Keywords: flexible monopile foundation, offshore wind turbine, pendulum tuned mass damper, power spectral density analysis, structural control

INTRODUCTION

Wind energy is one of the renewable sources in fast developing and implementation all over the world. Wind resources can be classified into onshore and offshore, covering, respectively, onshore and coastal installations. The Global Wind Energy Council (GWEC, 2020) reports that new installed wind power worldwide was 93.6 GW in 2021, reaching over 837 GW of total wind capacity, a growth of 12.4% compared to 2020. The offshore wind energy market in the year 2021 had a record year generating more than 21.1 GW, three times more than the previous year. Investors are now eyeing Brazil, reflected in applications for licensing more than 80 GW in offshore wind projects submitted to the Brazilian Institute for the Environment and Renewable Natural Resources (IBAMA). This is just a fraction of the technical resource potential in Brazil, which is over 700 GW, according to the EPE. The EPE also provides a conservative forecast that, by 2050, Brazil will reach 16 GW of offshore wind capacity installed at sea.

An offshore wind turbine is composed of a tower that receives excessive vibrations caused by the turbine and by the actions of the wind and sea currents, especially due to its slender geometry and great height. The analysis of the structural behavior of the tower is of great importance due to its cost, which can represent approximately 20% of the total cost of the system (Morais *et al.*, 2009). Tuned Mass Damper (TMD) is a widely used passive structural control (Housner *et al.*, 1997; Soong and Dargush, 1997; Elias and Matsagar, 2017). Briefly, it is a damper which transfers the kinetic energy from the main structure to a secondary mass usually. Extensive applications of passive devices coupled to wind turbines and OWTs have been investigated in the last years (Lackner and Rotea, 2011; Murtagh *et al.*, 2007; Ghassempour *et al.*, 2019). Murtagh *et al.* (2007) used as a passive controller to mitigate the vibration level of a simplified wind turbine model. Other authors present numerical models based on open-source FAST (NREL) (Stewart and Lackner, 2014; Park *et al.*, 2019). Applying optimization techniques, several authors define passive device parameters to maximize vibration mitigation (Bekdaş and Nigdeli, 2013; Pietrosanti *et al.*, 2020) The Pendulum Tuned Mass Damper (PTMD) is an alternative for TMD where the passive device is a pendulum (Park *et al.*, 2019; Resende *et al.*, 2020; Kecik and Mitura, 2020). Sun and Jahangiri (2018) developed an analytical model of the National Renewable Energy Lab (NREL) monopile 5-MW OWT coupled with a 3D-PTMD, under the misaligned wind, wave, and seismic loading. Deraemaeker and Soltani (2017) introduced an analytical procedure for the optimum design of a linear PTMD that was coupled to an undamped primary system, applying Den Hartog's equal peak method to derive the optimum design (Den, 1957). Tuning the PTMD consists of finding optimum values of stiffness and the damping function of both pendulum mass and length regarding a specific coupled system.

Some authors investigates the influence of the PSI using different tuned mass dampers (TMD) types (Brodersen *et al.*, 2016; Hussan *et al.*, 2018; Sun and Jahangiri, 2018), concluding that excluding the PSI effect could be the reason of overestimating the TMD performance (Hussan *et al.*, 2018). The aim of this study is investigating the PSI effects on a monopile of the NREL 5-MW OWT considering the PTMD by using static and dynamic analysis.

METHODOLOGY

Numerical global modeling of OWTs

The OWT is modeled using the FE method following some specifications of the Phase II (Monopile with Flexible Foundation) of the Offshore Code Comparison Collaboration (OC3) of the NREL 5-MW OWT, presented by Jonkman and Musial (2010). An integrated MATLAB®/ANSYS® APDL routine generates and evaluate the wave and wind rotational spectra, as well as the hydrodynamic and aerodynamic loads over the structure following the procedures adopt by Colherinhas *et al.* (2021) with some adaptations to consider the PSI described on the next subsection.

The aerodynamic loads follow the blade-element/momentum (BEM) theory and the rotating blades conditions are estimated by a power spectrum of a single blade root moment induced by turbulent wind velocity (Burton *et al.*, 2001), generating stochastic wind fields corresponding to a hub-height rated wind speed of 11.4 m/s. The Kaimal spectrum is used in conjunction with the Normal Turbulence Model (IEC, 2009) to produce the wind speed vectors along the tower. In across-wind direction, at certain critical ranges for the mean velocities, the frequency vortex shedding originating around the tower coincides with the first natural frequency of the lateral motion of the tower resulting in lock-in vibration, so a maximum across-wind displacement is applied in the tower to consider the lock-in effect.

The sea currents in shallow water follows a velocity field in which intensity decreases with depth (DNV, 2014) with a tidal and wind-generated current at the Mean Sea Level (MSL). For the wave dynamics, the particles' velocities and accelerations are computed by a linear Airy Theory for a wave height of $H_w = 6$ m and wave period of $T_w = 10$ s with a water depth of 20 meters. The wave loading are calculated using the Morison equation (Chakrabarti, 2005) with the sum of drag and inertia components, by applying the Airy wave theory. The Pierson-Moskowitz (PM) power spectrum is considered for the sea-surface elevation.

The tower geometry is modeled in ANSYS® APDL and the environmental actions are applied on the nodes, as shown Fig. 1, to perform a modal, spectral and static analysis. The auto- and cross-spectrum in force are inputs applied along the tower over the water nodes. The tower is modeled as BEAM188 elements and the monopile as PIPE288. The grout connection are neglected. The rotor-nacelle assembly (RNA) is modeled by two MASS21 elements: one for the hub and other for the nacelle, and they are connected through the shaft with a rigid connection (CERIG). The PSI model consists in 36×2 (p-y) nonlinear springs (each pair for a meter of pile depth) for both fore-aft (FA) and side-to-side (SS) directions, 36 (t-z) nonlinear springs for axial loads and one (Q-z) end bearing nonlinear spring. All spring are modeled with COMBIN39 elements related to the flexible foundation nodes.

The PTMD is modeled using a rigid connector (BEAM4) connected to a COMBIN14 torsional linear spring atop of the tower, then a mass (MASS21) is connected to the connector with a pendulum length (L_p). The PTMD is designed to be implemented in the turbine inside the tower and attached to the nacelle.

The dynamic structural response (r_p) are expressed in terms of its mean value (r_m) generated by the mean wind (including the vortex shedding effect on the tower) and by sea current and the response standard deviation (σ_r) related to the effects of turbulent wind and waves, using a response peak factor (g_r), as follows

$$r_p = r_m + g_r \cdot \sigma_r \tag{1}$$

For a complete non-linear analysis, the dynamic structural response is used in a static analysis to estimating the displacements and stresses of the flexible foundation.

Pile-Soil Interaction (PSI)

The geotechnical data applied in this study follows the realistic soil properties considered by the OC3 Phase II project for the 5-MW OWT (Jonkman and Musial, 2010), to modeling the flexible monopile foundation. The soil consists in a three-layers profile with soil density increasing with its depth. The effective soil weigh is $\gamma = 10.0$ kN/m^3 for the three layer. The first layer (from 0 to 5 meters depth) has angle of internal friction $\phi' = 33.0°$, the second (5 to 14 meters depth) $\phi' = 35.0°$, and the third (14 to 36 meters depth) $\phi' = 38.5°$, as shown Fig. 2 (a).

The most common and more accurate PSI model is the distributed springs (DS) model or Winkler foundation beam model, presented in Fig. 2 (b). The DS model is considered in this paper for representing the resistance of soil and consists in using lateral nonlinear springs (p-y) in along and across directions of the OWT, and axial nonlinear springs (t-z and Q-z). These springs supports the foundation, modeled as pipe elements with 1-meter equally separated nodes.

For construction of p-y curves, the type of soil, the type of loading, the remoulding due to pile installation and the effect of scour should be considered. The lateral soil resistance-deflection (p-y) relationships for sand are also non-linear and in the absence of more definitive information, the American Petroleum Institute (API, 2016) suggests the use of the following expression

$$p(y) = A p_u \tanh\left(\frac{kx}{A p_u} y\right) \tag{2}$$

where x is the position along the pile axis, y is the lateral displacements of the pile, k is the initial modulus of subgrade

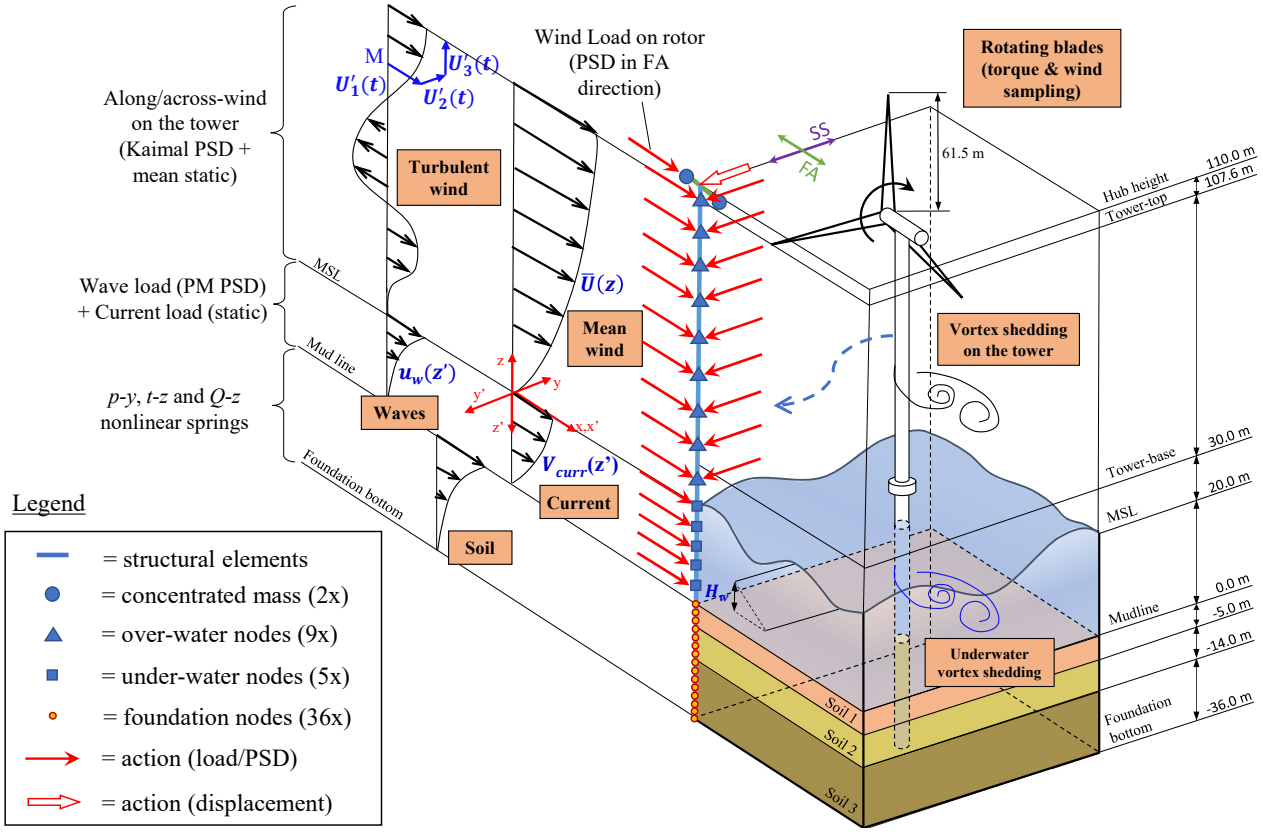

Figure 1 – OWT geometry and environmental actions over the nodes

reaction determined as function of angle of internal friction, ϕ', estimated from Fig. 3 (a) (API, 2016), and A is the factor to account cyclic or static loading condition, evaluated by

$$A = \begin{cases} 0.9 & \text{for cyclic loading} \\ \left(3.0 - 0.8\frac{x}{D}\right) & \text{for static loading} \end{cases} \tag{3}$$

The static ultimate lateral resistance per unit length p_u is the maximum value that p can take on when the pile is deflected laterally, estimated by the minimum value of the equations

$$p_u = \min \begin{cases} p_{us} = (C_1 x + C_2 D)\gamma x \\ p_{ud} = C_3 D \gamma x \end{cases} \tag{4}$$

where D is the average pile diameter from surface to depth, γ is the effective soil weight, and C_1, C_2, and C_3 are coefficients from Fig. 3 (b) in function of ϕ' (API, 2016).

A viscoelastic dashpot is placed in parallel with the lateral p-y springs, and the damping coefficient is determined as (Shi *et al.*, 2022)

$$c_m = k_s \frac{\beta_m}{\pi f_n} \tag{5}$$

where f_n is the first-order natural frequency of supporting structure [Hz], k_s is the secant stiffness [kN/m^2] of the (p-y) curve of Fig. 4 (a), β_m is the hysteretic damping ratio, taken as 5%.

For small displacements and distances between the springs, the secant stiffness values presented in Fig. 4 (b) are estimated considering the linearization of the (p-y) curve by the following equation (Wang *et al.*, 2013)

$$k_s = \frac{3}{y_x^3} \int_0^{y_x} p(y) y dy \tag{6}$$

This linearization of the monopile damping and stiffness is used to consider the effects of turbulent wind and waves in the spectral analysis.

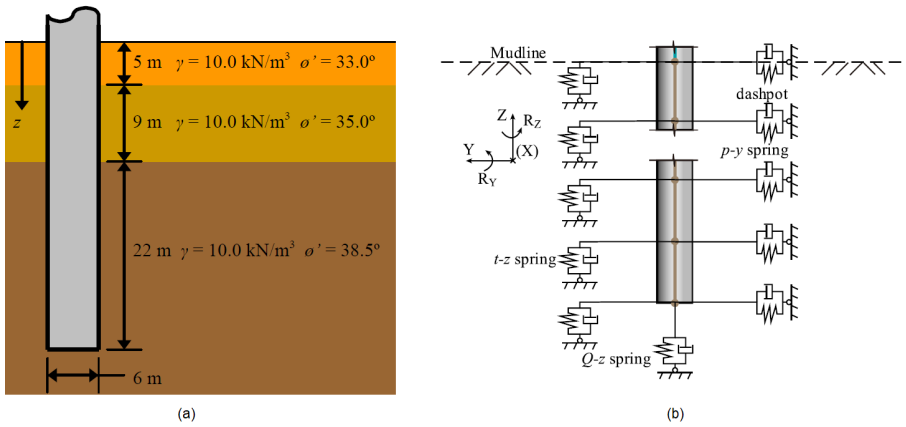

Figure 2 – (a) Soil Profile (Jonkman and Musial, 2010); (b) PSI model (Shi *et al.*, 2022)

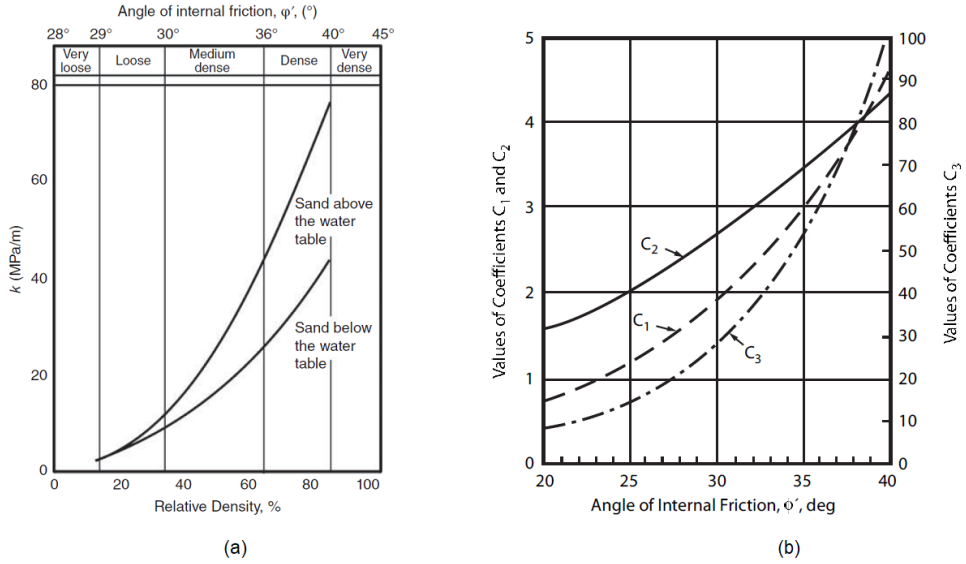

Figure 3 – (a) initial modulus of subgrade reaction k. (b) C_1, C_2, and C_3 coefficients; (API, 2016)

The pile capacity for axial bearing loads are computed in terms of the skin friction resistance and the total end bearing. The API (2016) provides theoretical-based curves for axial load transfer curves (t-z) and tip-load curves (Q-z) in function of the axial pile deflection (z), estimated for cohesionless soils (siliceous soil), respectively, in terms of the unit shaft friction f and the unit end bearing q as:

$$f = \beta p'_o \leq f_1 \tag{7}$$

$$q = N_q p'_o \leq q_1 \tag{8}$$

where β is the dimensionless shaft friction factor, N_q is the dimensionless bearing capacity factor, and p'_o is the effective overburden pressure at the depth in question. The unit skin friction capacity (f) and the unit end bearing (q) are limited by the upper limiting values of unit skin friction, f_1, and unit end bearing, q_1, respectively. The values for β, N_q, f_1, and q_1 are taken in function of the relative density and soil description, as shown Table 6.4.3 of the API (2016).

In this paper, the values adopted for the variables that constructs the (p-y), (t-z), and (Q-z) curves varies in function of the soil-pile friction angle (dense/ very dense), considering that the friction angle increases in function of the depth for the considered three-layers of the OC3 Phase II soil, taking the values of Tab. 1.

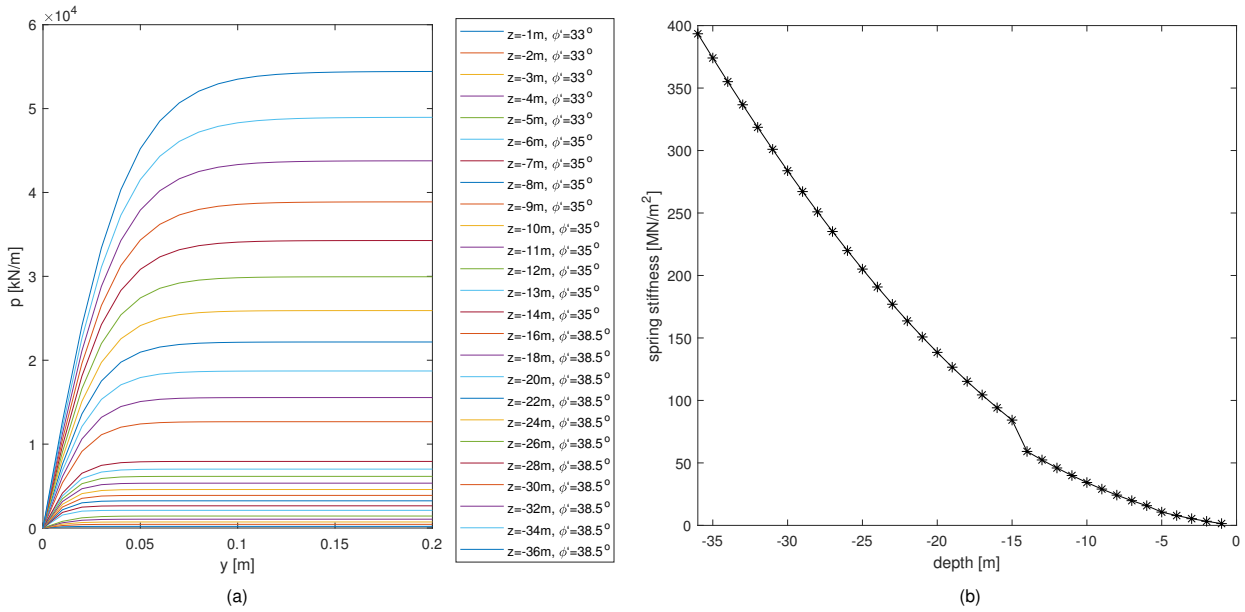

Figure 4 – (a) p-y curves; (b) secant stiffness'

Table 1 – Design parameters for lateral and axial resistance of driven piles in cohesionless soils

Angle of internal friction, ϕ' [°]	C_1 [-]	C_2 [-]	C_3 [-]	initial modulus of subgrade, k [MPa/m]	shaft friction factor, β [-]	limiting unit skin friction, f_1 [kPa]	end bearing factor, N_q [-]	limiting unit end bearing, q_1 [MPa]
33.0	2.5	3.2	40	18	0.46	96	40	10
35.0	3.0	3.5	55	33	0.50	110	45	11
38.5	4.0	4.0	80	36	0.56	115	50	12

RESULTS

From the results obtained by Colherinhas *et al.* (2021), a pre-selected optimal PTMD design case (DC) obtained from a Genetic Algorithm optimization, perform the results of this study considering the PSI. The torsional and the friction damping of the PTMD are considered as $K_p = 0.5$ kNm/rad and $C_p = 15.0$ kNms/rad, with a pendulum length of $L_p = 4.5$ m, and mass ratio between the pendulum and the tower of $\mu = 0.05$ (or pendulum mass $M_p = 44.88$ ton).

Table 2 presents a reduction of all natural frequencies between the OWT (with and without PTMD) with rigid foundation and considering PSI. These values are consistent when compared to the reference (Jonkman and Musial, 2010). Figure 5 shows graphically the shifting to the left of the tower-top PSD responses when considering the PSI for both OWT and OWT+PTMD configurations. The dynamic structure response decreases from 1.10 m to 0.90 m (18%) in FA direction and from 0.39 m to 0.34 m (13%) in SS direction, for the OWT with rigid foundation when coupling the PTMD. For the flexible foundation (with PSI) the response decreases from 1.58 m to 1.26 m (20%) in FA and from 0.57 m to 0.54 m (5%) in SS direction.

Table 2 – Natural frequencies for the OWT and OWT+PTMD models.

		Rigid Foundation		Flexible Foundation	
Mode		FA (Hz)	SS (Hz)	FA (Hz)	SS (Hz)
OWT	1st	0.275	0.275	0.254	0.255
	2nd	2.230	2.301	1.902	1.946
OWT+PTMD	1st	0.223	0.247	0.217	0.235
	2nd	0.292	0.316	0.277	0.309
	3rd	2.230	2.300	1.902	1.946

Figures 6 (a) and (b) shows the horizontal displacements in FA and SS direction, respectively, of the flexible foundation in function of the soil depth, presenting a 20% of displacement reduction in FA direction when the OWT is controlled by

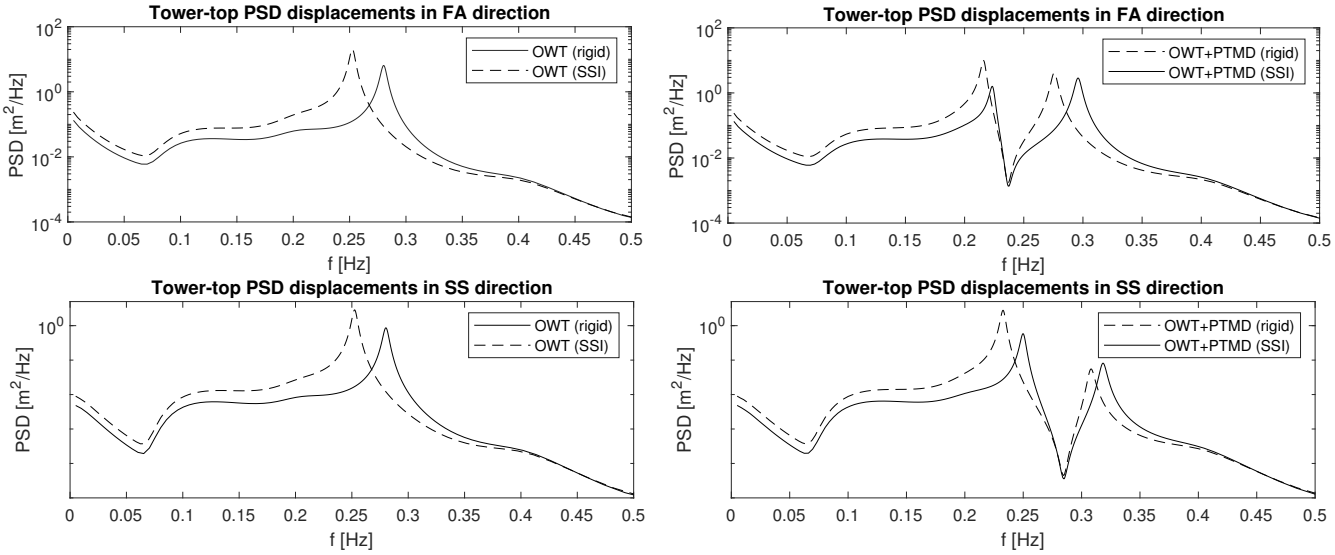

Figure 5 – PSD of tower-top displacements comparison for DC with and without foundation.

the PTMD. Figure 7 shows the axial axial and bending stresses acting in the pile. It's noticeable that the axial stresses increases when the PTMD is installed but the bending stresses decreases. A reduction from 156.80 MPa to 132.74 MPa (15%) of the stresses combined is reached when the PTMD controls the OWT.

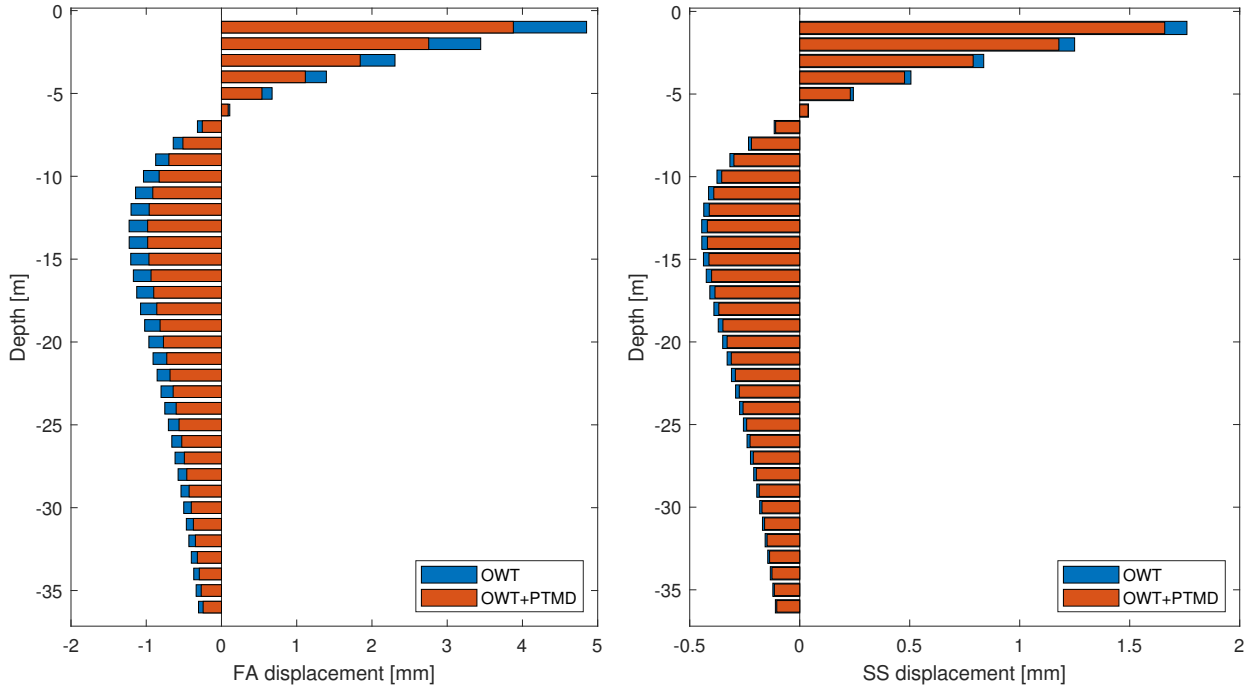

Figure 6 – Results from static analysis: FA (a) and SS (b) displacements

CONCLUSIONS

This study proposes a 3D-PTMD design to mitigate the vibration of OWTs in operational conditions considering the PSI effects over a flexible monopile foundation. The modal analysis presenting values near to the references when the PSI is considered for the NREL 5-MW OWT. When considering the PSI effects on a flexible monopile foundation the PSD

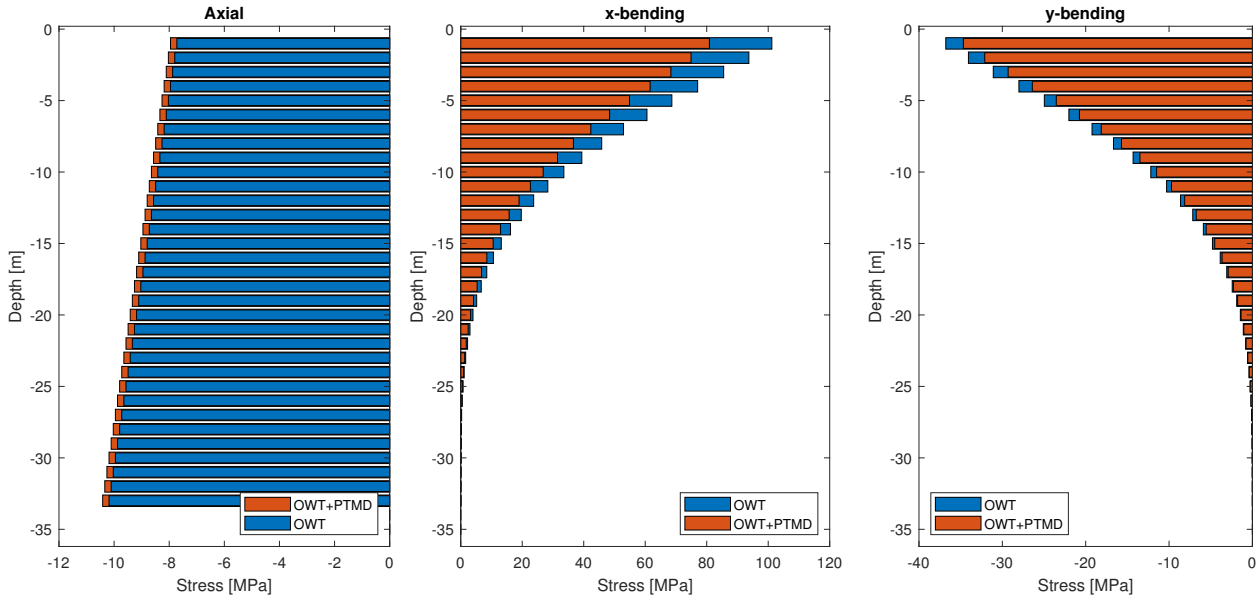

Figure 7 – Axial and bending stresses at the pile

analysis presents an increase of 30.4% in the FA direction and 28.6% in SS direction of the OWT tower-top response, in comparison to a rigid monopile (fixed at the seabed). It is noticed that the bending moments and the displacements on the foundation decreases due to the mitigating of the vibrations when the PTMD is installed.

For further studies the authors will: investigate more optimal PTMD configurations to reduce, even more, the tower-top responses; vary the wind velocity analyzing its effect over the tower-top response; improve the OWT model, considering the grout connection between the monopile and the tower; evaluate the uncertainty of the environmental and structural parameters for a multi-level structural modeling considering a performance-based design.

ACKNOWLEDGMENTS

The authors acknowledge the financial support of the *Eletrobras FURNAS Centrais Elétricas* and the *Programa de Pesquisa e Desenvolvimento Tecnológico* (P&D) of *ANEEL*.

REFERENCES

API, 2016. *Recommended Practice for Planning, Designing and Constructing Fixed Offshore Platforms—Working Stress Design*. American Petroleum Institute (API) Recommended Practice 2A-WSD (RP 2A-WSD), 21st edition.

Bekdaş, G. and Nigdeli, S.M., 2013. "Mass ratio factor for optimum tuned mass damper strategies". *International Journal of Mechanical Sciences*, Vol. 71, No. Supplement C, pp. 68 – 84. ISSN 0020-7403. doi:https://doi.org/10.1016/j.ijmecsci.2013.03.014. URL http://www.sciencedirect.com/science/article/pii/S0020740313000994.

Brodersen, M.L., Bjørke, A.S. and Høgsberg, J., 2016. "Active tuned mass damper for damping of offshore wind turbine vibrations". *Wind Energy*, Vol. 20, No. 5, pp. 783–796. doi:10.1002/we.2063. URL https://onlinelibrary.wiley.com/doi/abs/10.1002/we.2063.

Burton, T., David, S., Jenkins, N. and Bossanyi, E., 2001. *Wind energy: handbook*. J. Wiley. ISBN 9780471489979. URL https://books.google.it/books?id=m9dSAAAAMAAJ.

Chakrabarti, S., 2005. *Hadbook of Offshore Engineering - Volume 1*. Elsevier.

Colherinhas, G.B., Petrini, F., de Morais, M.V.G. and Bontempi, F., 2021. "Optimal design of passive-adaptive pendulum tuned mass damper for the global vibration control of offshore wind turbines". *Wind Energy*, Vol. 24, No. 6, pp. 573–595. doi:https://doi.org/10.1002/we.2590. URL https://onlinelibrary.wiley.com/doi/abs/10.1002/we.2590.

Den, H.J.P., 1957. "Mechanical vibrations. fourth edition. mcgraw-hill, new york, 1956. 67s. 6d." *The Journal of the Royal Aeronautical Society*, Vol. 61, No. 554, p. 139–139. doi:10.1017/S0368393100131049. URL https://doi.org/10.1017/S0368393100131049.

Deraemaeker, A. and Soltani, P., 2017. "A short note on equal peak design for the pendulum tuned mass dampers". *Proceedings of the Institution of Mechanical Engineers, Part K: Journal of Multi-body Dynamics*, Vol. 231, No. 1, pp. 285–291. doi:10.1177/1464419316652558. URL https://doi.org/10.1177/1464419316652558.

DNV, 2014. *Design of Offshore Wind Turbine Structures.* DNV-OS-J101 - Offshore Standard, Det Norske Veritas AS.

Elias, S. and Matsagar, V., 2017. "Research developments in vibration control of structures using passive tuned mass dampers". *Annual Reviews in Control*, Vol. 44, pp. 129–156. ISSN 13675788. doi:10.1016/j.arcontrol.2017.09.015. URL https://www.sciencedirect.com/science/article/pii/S1367578817301372.

Ghassempour, M., Failla, G. and Arena, F., 2019. "Vibration mitigation in offshore wind turbines via tuned mass damper". *Engineering Structures*, Vol. 183, pp. 610 – 636. ISSN 0141-0296. doi:https://doi.org/10.1016/j.engstruct.2018.12.092. URL http://www.sciencedirect.com/science/article/pii/S0141029618315220.

GWEC, 2020. "Global wind report annual market update 2020". Technical report, Technical Report, Global Wind Energy Council.

Housner, G.W., Bergman, L.A., Caughey, T.K., Chassiakos, A.G., Claus, R.O., Masri, S.F., Skelton, R.E., Soong, T.T., Spencer, B.F. and Yao, J.T.P., 1997. "Structural control: Past, present, and future". *Journal of Engineering Mechanics*, Vol. 123, No. 9, pp. 897–971. doi:10.1061/(ASCE)0733-9399(1997)123:9(897).

Hussan, M., Rahman, M.S., Sharmin, F., Kim, D. and Do, J., 2018. "Multiple tuned mass damper for multi-mode vibration reduction of offshore wind turbine under seismic excitation". *Ocean Engineering*, Vol. 160, pp. 449 – 460. ISSN 0029-8018. doi:https://doi.org/10.1016/j.oceaneng.2018.04.041. URL http://www.sciencedirect.com/science/article/pii/S0029801818305237.

IEC, 2009. *Wind turbines - Part 3: Design requirements for offshore wind turbines*. International Electrotechnical Commission (IEC) 61400-3, International Standard.

Jonkman, J.M. and Musial, W., 2010. *Offshore Code Comparison Collaboration (OC3) for IEA Task 23 Offshore Wind Technology and Deployment [electronic resource].* National Renewable Energy Laboratory. URL https://www.nrel.gov/docs/fy11osti/48191.pdf.

Kecik, K. and Mitura, A., 2020. "Energy recovery from a pendulum tuned mass damper with two independent harvesting sources". *International Journal of Mechanical Sciences*, Vol. 174, p. 105568. ISSN 0020-7403. doi:https://doi.org/10.1016/j.ijmecsci.2020.105568. URL http://www.sciencedirect.com/science/article/pii/S0020740319334459.

Lackner, M.A. and Rotea, M.A., 2011. "Passive structural control of offshore wind turbines". *Wind Energy*, Vol. 14, No. 3, pp. 373–388. ISSN 1099-1824. doi:10.1002/we.426. URL http://dx.doi.org/10.1002/we.426.

Morais, M.V.G., Barcelos, M., Ávila, S.M., Shzu, M.A.M. and de C. Silva, R., 2009. "Dynamic behavior analysis of wind turbine towers". In *CMN*. Congreso de Métodos Numéricos en Ingeniería, Barcelona, 29 junio al 2 de julio, España.

Murtagh, P.J., Ghosh, A., Basu, B. and Broderick, B.M., 2007. "Passive control of wind turbine vibrations including blade/tower interaction and rotationally sampled turbulence". *Wind Energy*, Vol. 11, No. 4, pp. 305–317. doi:10.1002/we.249. URL https://onlinelibrary.wiley.com/doi/abs/10.1002/we.249.

Park, S., Lackner, M.A., Pourazarm, P., Rodríguez Tsouroukdissian, A. and Cross-Whiter, J., 2019. "An investigation on the impacts of passive and semiactive structural control on a fixed bottom and a floating offshore wind turbine". *Wind Energy*, Vol. 22, No. 11, pp. 1451–1471. ISSN 1095-4244. doi:10.1002/we.2381. URL https://doi.org/10.1002/we.2381.

Petrini, F., 2009. *A probabilistic approach to Performance-Based Wind Engineering (PBWE).* Phd thesis/ dottorato di ricerca.

Pietrosanti, D., De Angelis, M. and Giaralis, A., 2020. "Experimental study and numerical modeling of nonlinear dynamic response of sdof system equipped with tuned mass damper inerter (tmdi) tested on shaking table under harmonic excitation". *International Journal of Mechanical Sciences*, Vol. 184, p. 105762. ISSN 0020-7403. doi:https://doi.org/10.1016/j.ijmecsci.2020.105762. URL http://www.sciencedirect.com/science/article/pii/S0020740320300539.

Resende, D.V., de Morais, M.V.G. and Avila, S.M., 2020. "Experimental Analysis of One-Degree-of-Freedom (1DoF) Dynamic System Controlled by Optimized Inverted Pendulum". *Journal of Vibration Engineering & Technologies*, p. 471–481. ISSN 2523-3920. doi:10.1007/s42417-020-00198-2. URL https://doi.org/10.1007/s42417-020-00198-2.

Shi, S., Zhai, E., Xu, C., Iqbal, K., Sun, Y. and Wang, S., 2022. "Influence of pile-soil interaction on dynamic properties and response of offshore wind turbine with monopile foundation in sand site". *Applied Ocean Research*, Vol. 126, p. 103279. ISSN 0141-1187. doi:https://doi.org/10.1016/j.apor.2022.103279. URL https://www.sciencedirect.com/science/article/pii/S0141118722002152.

Soong, T. and Dargush, G., 1997. *Passive Energy Dissipation Systems in Structural Engineering*. Wiley. ISBN 9780471968214. URL https://books.google.com.br/books?id=OxBmQgAACAAJ.

Stewart, G.M. and Lackner, M.A., 2014. "The impact of passive tuned mass dampers and wind–wave misalignment on offshore wind turbine loads". *Engineering Structures*, Vol. 73, pp. 54 – 61. ISSN 0141-0296. doi:http://dx.doi.org/10.1016/j.engstruct.2014.04.045. URL http://www.sciencedirect.com/science/article/pii/S0141029614002673.

Sun, C. and Jahangiri, V., 2018. "Bi-directional vibration control of offshore wind turbines using a 3d pendulum tuned mass damper". *Mechanical Systems and Signal Processing*, Vol. 105, pp. 338 – 360. ISSN 0888-3270. doi:https://doi.org/10.1016/j.ymssp.2017.12.011. URL http://www.sciencedirect.com/science/article/pii/S0888327017306465.

Wang, M., Zhao, Y., Du, W., He, Y. and Jiang, R., 2013. "Derivation and validation of soil-pile-interaction models for offshore wind turbines". Vol. All Days. International Ocean and Polar Engineering Conference: ISOPE-I-13-091.

RESPONSIBILITY NOTICE

The authors are the only responsible for the printed material included in this paper.